TRANSVERSE FAILURE UNDER COMPRESSION IN COMPOSITE LAMINATES: MICROSCOPICAL OBSERVATIONS.

P.L. Zumaquero, E. Correa, J. Justo and F. París

Group of Elasticity and Strength of Materiales, Continuum Mechanics Dpt., School of Engineering, Universidad de Sevilla, Camino de los Descubrimiento, s/n, 41092, Seville, Spain.

Email: pzumaquero@us.es

Keywords: Debonding; Transverse cracking; Micro-mechanics; Optical microscopy.

Abstract

Transverse failure is quite frequent in fibrous composite materials. This type of damage, known as Matrix/Inter-fibre failure at micromechanical level, is characterized by the appearance of small debonds at the fibre-matrix interfaces (interface cracks) that can progress along them until reaching a certain extension. From this point the interface cracks tend to change their directions and kink towards the matrix, growing through it and joining each other to finally provoke the failure of the material. Specially interesting is the study of this phenomenon when the material is submitted to compressive loads, due to the particular morphology of the interface cracks and the specific angle that the macro-cracks form in the matrix.

The previous numerical studies carried out at micro-mechanical level serve as the basis for the present work, whose objective is the study of transverse failure but from an experimental point of view. In particular, optical microscopy is used to identify different aspects of the failure such as the stages of damage, the extension of the interface cracks, the kinking angle and other types of damage that appears in coupons previously tested at different compressive loading levels.

1. Introduction

The study of the initiation of failure mechanisms in composite materials at micro-mechanical level is essential for the improvement of the existing criteria that predicts their appearance; the connection of the knowledge generated at this level with the macro-mechanical scale would contribute to a more accurate and efficient design of components made of composites.

The particular case of matrix/inter-fibre failure under compression, which corresponds, at the macro-mechanical level, to transverse failure under compression (i.e. failure occurring in 90º plies of multidirectional laminates or in unidirectional laminates subjected to transverse loads) has been analysed by several authors using numerical tools, see for instance Correa et al. [1-4],Vaughan and McCarthy [5], and Arteiro et al. [6]. In particular, the work by Correa et al. [1-4] identified the initial stages of the damage mechanism, and showed the importance of some key parameters on the progession of damage.

Specifically, as Figure 1 shows, the damage is assumed to initiate at the fibre-matrix interfaces as small (10º length) debonds (interface cracks) centred at 135º; these initial debonds (Stage I, Figure 1a)

present an interesting morphology characterized by an almost closed (contact) configuration with a small 'bubble' in their lower tip [1]. The debond growth along the interface (Stage II, Figure 1b) seems to be unstable until reaching a certain extension at the interface that coincides with the closing of the 'bubble'; this final amplitude of the crack at the interface is approximately 76º (corresponding to a position of the lower crack tip of 206º).

After this point, the interface crack growth turns stable, giving rise to Stage III of the damage mechanism, i.e. the kinking of the crack towards the matrix (Figure 1c). A very remarkable feature is that the crack does not kink into the matrix following an arbitrary orientation but an approximate angle of 53º with reference to the external load, coinciding with the macro-mechanical fracture angle detected experimentally (Figure 1d) and presumably formed by the coalescence of the aforementioned kinked cracks (named as Stage IV). This characteristic macro-mechanical failure angle has already been brought to light by other authors (see for instance Puck and Schürmann [7]).

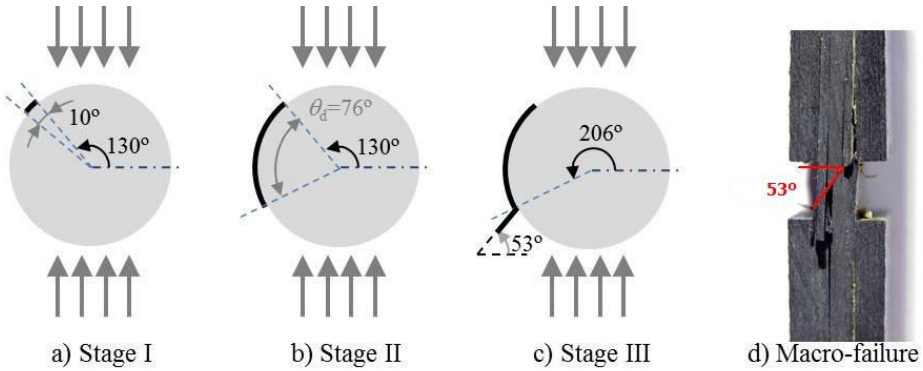

Figure 1. Stages of the inter-fibre failure under compression (Correa et al. [2]).

Based on the numerical studies performed by Correa et al. [1-4] on the behaviour of composites subjected to compressive transverse loads, this work focuses on the experimental identification of the different stages of the damage mechanism arising in coupons from 90º unidirectional and symmetrical cross-ply laminates subjected to compression and the measurement of the main parameters that define each stage.

2.Coupons manufacturing and testing

2.1 Coupons manufacturing

The coupons for compressive tests were manufactured based on ASTM D695-02a [8] and using a carbon/epoxy (Hexply AS4/8552) pre-preg. The corresponding reinforcing tabs were bonded using a standard epoxy film adhesive with a polyamide base (AF-163-2-K.06) from 3M.

Two different sets of coupons were manufactured: a first set from unidirectional 90º panels with 10 plies (and using the same laminate to build the tabs), Figure 2a; a second set from cross-ply symmetrical panels $[0_3, 90_3]_s$ with tabs from a $[0_{12}]$ laminate, Figure 2b.

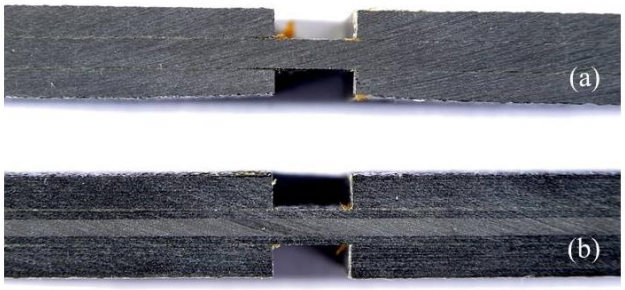

Figure 2. (a) Unidirectional coupon, (b) cross-ply coupon.

2.2 Transverse compressive tests

2.2.1. Unidirectional coupons

A first set of five unidirectional (UD) coupons was selected for testing under compression. The results obtained for the compressive strength (Y_c) showed a mean value of 279.8 MPa, a standard deviation of 4.8 MPa and a coefficient of variation of 1.7%, therefore implying an excellent result in terms of dispersion.

Then, subsequent testing campaigns were performed under maximum loads lower than the previously measured Y_c, in order to generate damage without reaching the catastrophic failure. In particular, the loads applied can be grouped in four levels: 25%Y_c, 50%Y_c, 75%Y_c and 80%Y_c, using six coupons for each group.

2.2.2. Cross-ply coupons

A similar procedure was employed in this case. A first set of five coupons was selected for testing under compression. The results obtained for the compressive strength of the laminate (X) showed a mean value of 883.7 MPa, a standard deviation of 23.9 MPa and a coefficient of variation of 2.7%, again implying and excellent result in terms of dispersion.

Subsequent testing campaigns were performed under maximum loads lower than the previously measured X, aiming to generate damage at the 90º layer without reaching the catastrophic failure of the whole laminate. In particular, the loads applied can be grouped in four levels: 70%X (1 coupon), 75%X (6 coupons), 90%X (6 coupons) and 95%X (5 coupons).

3. Microscopical inspections

Before the microscopical observation it was necessary to prepare the coupons for the inspection. This preparation consisted on the inlay of the central part of the coupons with the help of a mould and then the samples were sanded and polished. The result of the polishing process must allow the fibres corresponding to the 90° plies to be clearly observed in an optical microscope at 1000x magnification.

The microscopical inspection has been made using an optical microscope *Eclipse MA100* from Nikon and *Perfect Image V8.01* software for the acquisition and edition of pictures.

3.1. Macro-cracks

For the unidirectional coupons, macro-cracks visible at low magnification (25x) only appeared at the group of coupons tested to failure. Nevertheless, it was possible to find some macro-cracks (Stage IV) visible at high magnification (1000x) in coupons tested at 50% Y_c and 80%Y_c.

In the case of cross-ply coupons, and as happened with the unidirectional coupons, the microscopical observation revealed again that only coupons tested until breakage showed macro-cracks visible at low magnification. At loading levels close to the laminate strength (90%X and 95%X) some macro-cracks were detected at high magnification.

3.2. Stages and other damages observed

As explained in Section 1, taking the numerical predictions from Correa et al. [1-4] as a reference, the different stages of the mechanism of damage need to be microscopically identified.

First of all, it is important to highlight that the three initial stages (Figure 1) were observed at all loading levels lower than Y_c in the unidirectional coupons, but they were more difficult to identify in the cross-ply coupons, where, for instance, Stage I was only detectable at 95%X. Figure 3 contains an example of each stage.

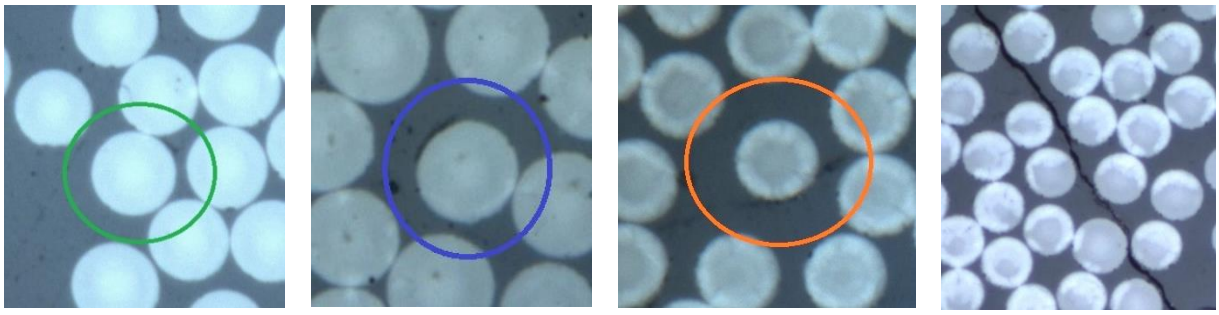

(a) (b) (c) (d)

Figure 3. (a) Stage I (UD coupon, 25%Y_c), (b) Stage II (UD coupon, 50%Y_c), (c) Stage III (UD coupon, 50%Y_c), (d) Stage IV (UD coupon, 100%Y_c).

In addition to the stages predicted by the previous numerical studies, other types of damage were detected in both unidirectional and cross-ply coupons: Damage V: Hole in the matrix (Figure 4a); Damage VI: Crack tangent to one or several fibres (Figure 4b); Damage VII: Crack touching a point of a fibre (Figure 4c); and Damage VIII: Crack in the matrix (Figure 4d).

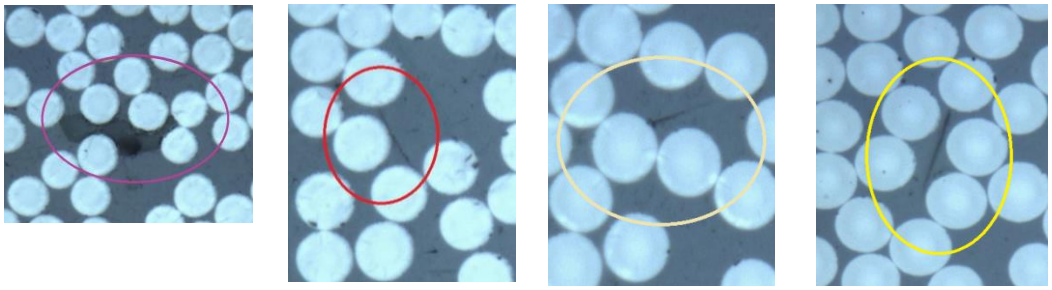

(a) (b) (c) (d)

Figure 4. Other types of damage: (a) Hole (UD coupon, 80%Y_c), (b) Tangent crack (UD coupon, 80%Y_c), (c) Crack touching a fibre (UD coupon, 25%Y_c), (d) Matrix crack (UD coupon, 50%Y_c).

3.2.1. Unidirectional coupons

In the case of unidirectional coupons, the total number of imperfections (Stages I to IV and other types of Damage, V to VIII) encountered at each loading level were 182 for 25%Y_c, 130 for 50%Y_c, 66 for 75%Y_c and 117 for the 80%Y_c case. In Table 1 the type of imperfection and its percentage of appearance for each loading level are detailed.

The information presented in Table 1 leads to the conclusion that the types of Damage VI, VII and VIII prevail at all loading levels. In contrast (and as mentioned in the previous Section) Stage IV is only present in coupons tested at 50%Y_c and 80%Y_c. The remaining stages are localized at all loading levels.

Table 1. Imperfections at unidirectional coupons.

	25%Y_c	50%Y_c	75%Y_c	80%Y_c
Stage I	4.9%	2.3%	1.5%	0.8%
Stage II	2.7%	4.6%	3.0%	2.6%
Stage III	1.7%	3.1%	1.5%	4.3%
Stage IV	0%	1.5%	0%	1.7%
Damage V	4.4%	3.1%	24.3%	12.8%
Damage VI	34.1%	44.6%	36.4%	34.2%
Damage VII	13.7%	10.8%	1.5%	11.1%
Damage VIII	38.5%	30.0%	31.8%	32.5%

3.2.2. Cross-ply coupons

The total number of imperfections counted at each loading level of cross-ply coupons were 49 for 70%X, 17 for 75%X, 100 for 90%X and 116 for 95%X. Some of the coupons tested under 95%X were necessary polished twice because the first polish was considered to be insufficient (showing some polishing marks and remains). This group was called 95%X(b), and in this case 296 imperfections were identified.

As can be observed in Table 2, at all loading levels the types of Damage VI and VIII prevail. In contrast, Stage I is only present at 95%X and after the second polishing process (95%X (b)), where a greater number of imperfections were counted.

Table 2. Imperfections at cross-ply coupons.

	70%X	75%X	90%X	95%X	95%X (b)
Stage I	0%	0%	0%	0%	2.3%
Stage II	4.1%	0%	4.0%	6.0%	5.8%
Stage III	6.1%	5.9%	0%	4.3%	5.0%
Stage IV	0%	0%	3.0%	7.8%	0.7%
Damage V	16.3%	23.5%	29.0%	13.8%	10.5%
Damage VI	28.6%	11.8%	32.0%	30.2%	42.9%
Damage VII	0%	0%	0%	8.6%	9.5%
Damage VIII	44.9%	58.8%	32.0%	29.3%	23.3%

Finally, from the comparison of unidirectional and cross-ply samples it is concluded that Stage I is more frequently observed and at lower loading levels in the unidirectional coupons. Stage IV is more common in cross-ply coupons, a fact that may be associated with the constraining effect of the 0º layer, which may allow the generation of a greater number of macro-cracks in the 90º layer before the complete failure of the coupon. Conversely, in unidirectional coupons failure occurs due to unstable propagation of one of these macro-cracks quickly after their formation.

3.3. Measurement of Stage II debond extension

Another interesting point of study is the measurement of the final extension of the crack at the interface (Stage II) that gives rise to Stage III (represented by the debonding angle θ_d in Figure 1). These measurements have been carried out on macro-cracks visible at low magnification, in particular in those samples from coupons tested until breakage.

The numerical study, Correa et al. [1-4], predicted that the final lenght of the interface crack at an isolated fibre is approximately 76°. In this work, no isolated fibres with macro-cracks were located, instead, it was considered the case of partially isolated fibres, Figure 5.

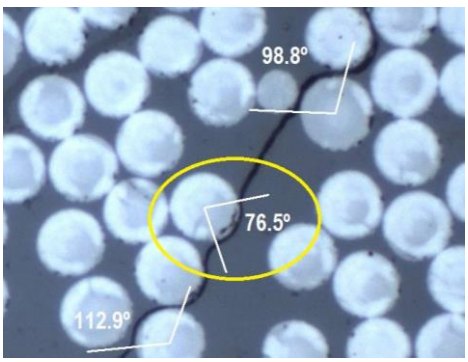

Figure 5. θ_d measures in partially isolated and non-isolated fibres.

It was possible to measure 24 interface cracks on partially isolated fibres in unidirectional coupons and 50 in the cross-ply group. Notice the difficulty in finding partially isolated fibres in real laminates with a high fibre volume content.

Table 3 presents the θ_d measurements divided in sub-ranges (in percentage of appearance) for both groups of samples. From the results it can be deduced that the amplitudes in the 70º-80º range prevail for both groups of specimens, in agreement with Correa et al. [1,2].

Table 3. θ_d distribution and percentage of appearance in partially isolated fibres.

θ_d	90_{10}	$[0_3, 90_3]_s$
<60°	29.2%	18.0%
60°-70°	8.3%	10.0%
70°-80°	33.3%	26.0%
80°-90°	16.7%	12.0%
90°-100°	12.5%	10.0%
>100°	0%	24.0%

3.4 Measurement of the kinking angle

As it was explained in Section 1, the orientation of the failure plane in coupons tested under transverse compression is commonly around 53º-55º. The numerical studies performed by Correa et al. [1-4] using single-fibre models showed that the numerically predicted kinking angle of the crack into the matrix (Stage III, Figure 1c) coincided with this experimental angle, thus showing a connection between the micro-numerical level and the macro-experimental level.

At this point it seems crucial to check if the experimental observations carried out in this work allow connecting the numerical and experimental approaches at micro-mechanical level.

With this aim in mind, measurements of the kinking angle in macro-cracks of coupons tested until breakage have been performed. A predominant range of 50º-60º arises (in agreement with [3]) although kinking angles outside this range were also measured. Moreover, many examples of cracks that kink into the matrix following an orientation between 53º and 55º have been found, which in fact is the prevailing sub-range within the aforementioned 50º-60º range. Figure 6 demonstrates this fact showing an interface crack kinking into the matrix following an orientation of ~54.5º.

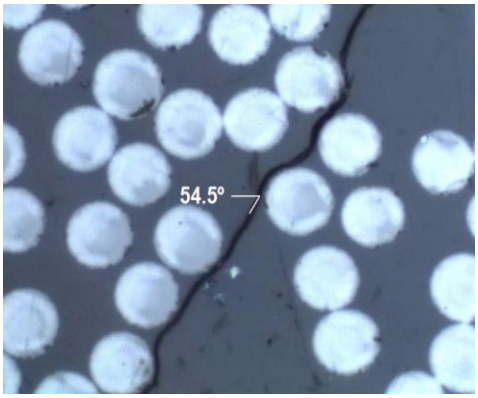

Figure 6. Measurement of the kinking angle.

5. Conclusions

This work focuses on the experimental identification of the different stages of the inter-fibre failure under compression in carbon-epoxy coupons by means of optical microscopy. Crucial parameters, such as the interface crack length that gives rise to the kinking towards the matrix and the kinking angles, have been measured. The experimental values agree with the previous numerical predictions.

Acknowledgements

This work was supported by the Spanish Ministry of Education, Culture and Sports under Grants MAT2016-80879-P and MAT2013-45069-P.

References

[1] E. Correa, F. París, V. Mantič. Numerical characterisation of the fibre-matrix interface crack growth in composites under transverse compression. *Engineering Fracture Mechanics*, 75:4085-103, 2008.
[2] E. Correa, F. París, V. Mantič. A micromechanical view of inter-fibre failure of composite materials under compression transverse to the fibres. *Composites Science and Technology*, 68:2010-21, 2008.
[3] E. Correa, F. París, V. Mantič. BEM analysis of inter-fibre failure under compression in composites: comparison between carbon and glass fibre systems. *Plastics, Rubber and Composites*, 40(6/7):333-41, 2011.
[4] E. Correa, F. París, V. Mantič. Effect of thermal residual stresses on the matrix failure under transverse compression at micromechanical level-a numerical and experimental study. *Composites Part A-Applied Science and Manufacturing*, 43:87-94, 2012.
[5] T.J. Vaughan, C.T. McCarthy. Micromechanical modelling of the transverse damage behaviour in fibre reinforced composites. *Composites Science and Technology*, 71(3):388-96, 2011.
[6] A. Arteiro, G. Catalanotti, A.R. Melro, P. Linde, P.P. Camanho. Micro-mechanical analysis of the effect of ply thickness on the transverse compressive strength of polymer composites. *Composites Part A-Applied Science and Manufacturing*, 79:127-37, 2015.
[7] A. Puck, H. Schürmann. Failure analysis of FRP laminates by means of physically based phenomenological models. *Composites Science and Technology*, 58(7):1045-67, 1998.
[8] ASTM D695-02a. Standard Test Method for Compressive Properties of Rigid Plastics, West Conshohocken, PA: ASTM International; 2003.